

Article (refereed) - postprint

Zhong, Jun; Li, Si-Liang; Ding, Hu; Lang, Yunchao; Maberly, Stephen C.; Xu, Sheng. 2018. **Mechanisms controlling dissolved CO₂ over-saturation in the Three Gorges Reservoir area** [in special issue: Effects of dams on river biogeochemistry and ecology] *Inland Waters*, 8 (2). 148-156.
<https://doi.org/10.1080/20442041.2018.1457848>

© 2018 International Society of Limnology (SIL)

This version available <http://nora.nerc.ac.uk/id/eprint/520643/>

NERC has developed NORA to enable users to access research outputs wholly or partially funded by NERC. Copyright and other rights for material on this site are retained by the rights owners. Users should read the terms and conditions of use of this material at
<http://nora.nerc.ac.uk/policies.html#access>

This is an Accepted Manuscript of an article published by Taylor & Francis Group in *Inland Waters* on 14/06/2018, available online:
<https://doi.org/10.1080/20442041.2018.1457848>

Contact CEH NORA team at
noraceh@ceh.ac.uk

1 **Mechanisms controlling dissolved CO₂ over-saturation in the Three**
2 **Gorges Reservoir area**

3 Jun Zhong,¹ Si-Liang Li,^{1,2*} Hu Ding,³ Yunchao Lang,¹ Stephen C. Maberly,⁴ and
4 Sheng Xu⁵

5 ¹ Institute of Surface-Earth System Science, Tianjin University, Tianjin 300072, China

6 ²State Key laboratory of Hydraulic Engineering Simulation and Safety, Tianjin University, Tianjin
7 300072, China

8 ³The State Key Laboratory of Environmental Geochemistry, Institute of Geochemistry, Chinese
9 Academy of Sciences, Guiyang 550081, China

10 ⁴Lake Ecosystems Group, NERC Centre for Ecology & Hydrology, Lancaster Environment Centre,
11 Lancaster LA1 4AP, UK

12 ⁵Scottish Universities Environmental Research Centre, East Kilbride, G75 0QF, UK

13

14 *Corresponding author: Email, siliang.li@tju.edu.cn

15 Fax, 0086 22 27405053

16

Mechanisms controlling dissolved CO₂ over-saturation in the Three Gorges Reservoir area

Abstract: The loss of CO₂ to the atmosphere from inland waters is an important part of the global carbon cycle. The Three Gorges Dam is the largest hydraulic project in the world and has consequently been widely studied. Here, we made spatially and temporally comprehensive measurements of partial pressure of CO₂ (*p*CO₂) variability along the Three Gorges Dam system. The *p*CO₂ ranged from 619 to 2383 μ atm for the collected samples, and were supersaturated relative to atmospheric CO₂. At the station near the upstream part of the reservoir, the *p*CO₂ at high-flow was much lower than that at low-flow. In contrast, *p*CO₂ at high-flow is much higher than that in the low-flow for the waters in front of the dam and after the dam. Rates of organic matter mineralization increased at high-flow, which produced increased *p*CO₂ in the surface water of the reservoir area. Mineralization of organic carbon should be responsible for the $\delta^{13}\text{C}$ -depleted of riverine DIC. Organic carbon mineralization is sensitive to temperature variability, and temperature is expected to be an important driver of the dissolved CO₂ over-saturation. The construction of Three Gorges Reservoir increased the water transit time and accelerated the organic carbon mineralization in Three Gorges Reservoir. The results suggest that carbon cycling changes markedly in large rivers that have been impounded.

Keywords: *p*CO₂, Three Gorges Reservoir, organic carbon mineralization, $\delta^{13}\text{C}_{\text{DIC}}$, temperature sensitivity

38 **Introduction:** Inland waters link terrestrial and oceanic ecosystems by transporting
39 materials from land to ocean (Barth et al., 2003; Wang et al., 2014b) and also
40 exchange material with the atmosphere (Kosten et al., 2010; Raymond et al., 2013).
41 Although the fluvial carbon export by inland water only occupies a small portion
42 (10^{15} g C year⁻¹) of the global carbon cycle (Aucour et al., 1999; Meybeck, 1982), it
43 plays an important role in regional carbon cycling (Wang et al., 2014b). However, in
44 the last few decades, the natural fluvial processes in many rivers have been disturbed
45 by anthropogenic activities (Guo et al., 2015; Humborg et al., 1997; Raymond et al.,
46 2008; Regnier, 2013), and the consequences of dam construction have been
47 intensively studied (Bao et al., 2014; Barros et al., 2011; Humborg et al., 1997; Wang
48 et al., 2014a; Wang et al., 2013; Wang et al., 2011). Impoundment converts a river into
49 an “artificial lake”, and consequently modifies the ecological function and
50 biogeochemical processes of the inland water. River regulation by dam construction
51 has become an important environmental problem affecting greenhouse gas release
52 from rivers although hydropower is regarded as a “green energy” (Chen et al., 2011;
53 Humborg et al., 1997; Wang et al., 2011). Enhanced dam construction in rivers has
54 greatly changed the transport of sediment, dissolved silica and terrestrial organic
55 carbon (Bao et al., 2014; Humborg et al., 1997; Yang et al., 2015; Yang et al., 2007a;
56 Yang et al., 2007b; Yu et al., 2011). The construction of dams would moderate the
57 organic matter fluxes and compositions downstream, and the trapping of sediment
58 within a reservoir would result in intensive respiration, thus increasing the proportion
59 of aquatic carbon, as well as CO₂ emission from inland waters (Bao et al., 2014).

60 The Three Gorges Dam is the largest hydropower dam in the world, and the
61 ecological environment and biogeochemical processes in the Three Gorges Reservoir
62 have been widely studied (e.g. Bao et al., 2014; Yang et al., 2007b; Zhang et al., 2014).
63 Previous studies have estimated the changes in hydrology and sediment dynamics in
64 the Three Gorges Reservoir (Dai and Liu, 2013; Deng et al., 2016; Li et al., 2016; Xu
65 and Milliman, 2009; Yang et al., 2015), biogeochemistry (Bao et al., 2014; Mao et al.,
66 2017) and greenhouse gases emissions (Chen et al., 2011; Zhao et al., 2013). However,
67 few studies have focused on the sources of the dissolved CO₂ and the relative
68 biogeochemical processes in inland waters. Artificial reservoirs are known to be
69 potential CO₂ contributors to the atmosphere (Raymond et al., 2013; Wang et al.,
70 2015). Dissolved CO₂ over-saturation with respect to the atmosphere is the main
71 driver of CO₂ emissions. Multiple control mechanisms have been proposed for the
72 CO₂ over-saturation in inland waters. Maberly et al. (2013) found that catchment
73 productivity controls CO₂ emissions for lakes. Marcé et al. (2015) showed that
74 carbonate weathering is a driver of CO₂ over-saturation in lakes. Inorganic carbon
75 loading was regarded as a primary driver of dissolved CO₂ concentrations in lakes and
76 reservoirs of the contiguous United States (McDonald et al., 2013). Ward et al. (2013)
77 found that degradation of terrestrial macromolecules contributes significantly to CO₂
78 out-gassing from inland waters.

79 In this study we investigated the temporal and spatial patterns of dissolved
80 inorganic carbon (DIC), dissolved organic carbon (DOC), particulate organic carbon
81 (POC), the partial pressure of CO₂ ($p\text{CO}_2$) and stable carbon isotope of DIC ($\delta^{13}\text{C}_{\text{DIC}}$)

82 in surface water of the Three Gorges Reservoir area. The objectives of the study are to:
83 (1) investigate the carbon dynamics in the Three Gorges Reservoir, (2) trace the main
84 sources of the dissolved CO₂ in the Three Gorges Reservoir, (3) analyze the
85 controlling mechanisms of the dissolved CO₂ over-saturation.

86

87 **Study site**

88 As the largest hydropower project in the world, the Three Gorges Reservoir
89 (TGR, Fig. 1) is located between the upper and middle reaches of the Changjiang
90 River, upstream of Yichang city in Hubei province (Deng et al., 2016; Zhao et al.,
91 2013). Three Gorges Reservoir is a narrow V-shaped valley-type reservoir with steep
92 slopes of the river channel. Mountainous areas occupy up to 96% of the Three Gorges
93 Reservoir area, with 4.3% plain area only in the river valley (Zhao et al., 2013). The
94 Three Gorges Reservoir experiences a humid subtropical monsoon, with an annual
95 mean temperature of 18°C (Mao et al., 2017). The local annual rainfall is
96 approximately 1250 mm and occurs mainly from May to September (Mao et al.,
97 2017).

98 The Three Gorges Reservoir has been fully operational since the end of 2008
99 (Zhao et al., 2013). The water level ranges from 145 m at high-flow to control floods
100 and 175 m at low-flow to retain water, with corresponding storage capacities of 17.2
101 and 39.3 km³, respectively (Yang 2014). High-flow is defined as from May to October
102 and low-flow as from November to April of the subsequent year, based on water
103 regulation at the Three Gorges Reservoir, according to the water level.

104

105 **Methods**

106 Six sampling sites (QX, WZ, ZZ, TPX, HL and YC) were chosen in the Three
107 Gorges Reservoir area (Fig. 1), of which four sampling sites (QX, TPX, HL and YC)
108 were chosen for long-term observation. QX is located near the inflowing water of the
109 reservoir, WZ, ZZ and TPX are located sequentially down-stream within the reservoir
110 and HL and YC are located downstream of the water discharged from the Three
111 Gorges Reservoir and Gezhou dams, respectively. We collected samples at QX,
112 monthly, for two hydrological years, and added extra sampling occasions during
113 high-flow. TPX, HL and YC were sampled, monthly, for a hydrological year, and
114 additional samples were added during high-flow.

115 Water temperature (T), pH and Electric Conductivity (EC) were measured
116 directly at the time of sampling for the surface water using a portable EC/pH meter
117 (WTW, pH 3210/Cond 3210 Germany). Water samples were collected in sealed high
118 density polyethylene (HDPE) bottles and the alkalinity was measured by Gran
119 titration with 0.02 M HCl within 24 hours of sampling. The concentration of DOC
120 was analyzed using an OI Analytical Aurora 1030 TOC analyzer. Total suspended
121 solids (TSS) were trapped on a glass-fibre filter paper (0.7 μ m, Whatman, GF/F) and
122 then freeze dried and weighed. Particulate organic carbon (POC) was measured with
123 an elemental analyzer (PE2400 (II), Perkin Elmer) after acidification. The $\delta^{13}\text{C}_{\text{DIC}}$
124 was determined by the method of Li et al., (2010), 20 ml aliquots of water were
125 purified on a vacuum line with 2 ml 85% phosphoric acid and magnetic stir bars, with

126 a precision of 0.2 ‰. Daily water discharge and water level data were obtained online
127 from the Ministry of Water Resources (<http://www.hydroinfo.gov.cn/>). The $p\text{CO}_2$ was
128 calculated based on mass balance relationships and the relative equilibrium constants.

129

130 **Results**

131 Hydrological characteristics

132 Although the Changjiang River carries a tremendous volume of water, the Three
133 Gorges Dam can moderate the downstream delivery of water. The water level ranged
134 from 145 m to 175 m above the sea level in the study period (Fig. 1). The Changjiang
135 river water is retained in the Three Gorges Reservoir in the low-flow season, and the
136 water level is kept at a relatively high level to meet water navigation and hydropower
137 requirements (Fig. 1). The water level is decreased to a low level from April to June,
138 to provide capacity for flood control (Fig. 1). From September to October, the water
139 level is increased to impound water, and a high level is maintained during the dry
140 season (Fig. 1). At QX, in the upper reaches of the reservoir, discharge varied from
141 4293 to 36484 m^3s^{-1} , with an average of 10242 m^3s^{-1} from February 2015 to February
142 2016. Because of the water regulation, discharge is less variable at HL and YC: from
143 5050 to 31800 m^3s^{-1} and from 5620 to 32600 m^3s^{-1} , respectively. However, the
144 average discharge was not significantly different at the three hydrological stations,
145 indicating that the contribution of other inflowing rivers is minor.

146

147 Variations of carbon species and $\delta^{13}\text{C}_{\text{DIC}}$ in the TGR

148 The range of temporal variations of water environment variables was much
149 larger than that of spatial variation. Temperature varied seasonally from 11.2 to 28.9□
150 and there was little variation between water temperature in the surface water of the
151 reservoir (TPX) and the discharged water at HL. This is markedly different to other
152 reservoirs (Wang et al., 2014b), which may be caused by the weak stratification in the
153 Three Gorges Reservoir (Wu et al., 2012). The pH value varied from 7.75 to 8.31 for
154 all the samples, with little spatial variation. Conductivity varied from 295 to 410
155 μScm^{-1} , with both the maximum and minimum values observed in QX. The more
156 stable status of the other sites could be ascribed to the regulating effect of the Three
157 Gorges Reservoir. DOC ranged from 0.86 to 2.05 mgL^{-1} , again with lower spatial
158 variation than temporal variation. Alkalinity ranged from 1.97 mequivL^{-1} to 2.60
159 mequivL^{-1} , and the alkalinity at QX was higher than at other stations. The $p\text{CO}_2$
160 ranged from 619 to 2383 μatm (Fig. 2a), and so all the samples are supersaturated
161 relative to atmospheric CO_2 and hence sources to the atmosphere. The $p\text{CO}_2$ values of
162 samples in WZ and ZZ are between that of QX and TPX in January, 2016. The $p\text{CO}_2$
163 values decreased from QX to YC in the low-flow season, and increased in the
164 high-flow season (Fig. 2a). The $p\text{CO}_2$ values were higher in the low-flow season
165 ($1150 \pm 343\mu\text{atm}$) than in the high-flow season ($987 \pm 309 \mu\text{atm}$) at QX, but the $p\text{CO}_2$
166 values were lower in the low-flow season at the other sites (Fig. 2a). The $p\text{CO}_2$ in the
167 reservoir area is always lower than in the inflowing water and the out-flowing water
168 in reservoirs of Southwest China. However, Similar $p\text{CO}_2$ values between reservoir
169 area and the out-flowing water were occurred for TGR (Fig. 2a). The $\delta^{13}\text{C}_{\text{DIC}}$ varied

170 from -13.2‰ to -6.6‰ for all the samples, and the $\delta^{13}\text{C}_{\text{DIC}}$ of QX was much heavier
171 than at other stations, especially at high-flow (Fig. 2b). The $\delta^{13}\text{C}_{\text{DIC}}$ values were lower
172 in the high-flow season at all sites.

173

174 **Discussion:**

175 Response of $p\text{CO}_2$ and $\delta^{13}\text{C}_{\text{DIC}}$ to hydrological change

176 Emissions of CO_2 from the water to the atmosphere have been explored in
177 relation to CO_2 sources and processes (Whitfield et al., 2010) including soil CO_2
178 discharge, *in situ* degradation of organic carbon, CO_2 degassing rates, carbonate
179 weathering, inorganic carbon loading and photosynthesis (Johnson et al., 2008;
180 Larsen et al., 2011; Li et al., 2010; Maberly et al., 2013; Marcé et al., 2015;
181 McDonald et al., 2013). There is a negative correlation between $p\text{CO}_2$ and discharge
182 near the upper reaches of the reservoir at QX (Fig. 3a), indicating a dilution effect by
183 overland flow at high-flow. $p\text{CO}_2$ was lower in high-flow than in low-flow, but $p\text{CO}_2$
184 was variable in both seasons (Fig. 3a) indicating that hydrological variation is not the
185 main controller of $p\text{CO}_2$ at QX, and other effects are important. The negative
186 correlation between $p\text{CO}_2$ and discharge shows that $p\text{CO}_2$ exhibits strong
187 biogeochemical stationarity (relatively stable behavior in response to changing
188 discharge). Soil CO_2 discharge or degradation of organic matters may be responsible
189 for this biogeochemical stationarity with high-discharge, which is similar to studies in
190 Wujiang (Zhong et al., 2017).

191 There was a large dynamic range of $\delta^{13}\text{C}_{\text{DIC}}$ values at QX, with a minimum at the

192 high-flow and a maximum at the low-flow (Fig. 3b). The $\delta^{13}\text{C}_{\text{DIC}}$ was negatively
193 correlated to the discharge for QX (Fig. 3b). Negative $\delta^{13}\text{C}_{\text{DIC}}$ values were related to
194 higher discharge, which should not be ascribed to simple dilution. High
195 concentrations of CO_2 derived from terrestrially fixed carbon broken down in the soil
196 can enter the water directly (Maberly et al., 2013). Large amounts of soil CO_2 were
197 discharged into the river during high discharge, producing more negative $\delta^{13}\text{C}_{\text{DIC}}$
198 values in the water (Li et al., 2010; Zhong et al., 2017). Mineralization of
199 macromolecules in the channel can also produce lighter $\delta^{13}\text{C}_{\text{DIC}}$ values in the water
200 (Ward et al., 2013). Soil CO_2 recharge is likely to be the main driver of CO_2 dynamics
201 responding to hydrological variation in QX (Zhong et al., 2017).

202 A negative relation between $p\text{CO}_2$ and discharge occurred at QX (Fig. 3a),
203 however, there were positive relationships between $p\text{CO}_2$ and discharge at HL and YC
204 (Fig. 4a), both of which are located downstream of the TGD. The positive relationship
205 contrasts to the relationship at QX (Fig. 3a), with no dilution occurring in the
206 high-flow season at HL and YC (Fig. 4a). Higher values of $p\text{CO}_2$ were recorded with
207 high discharge, which is contrary to QX, ascribing to multiple biogeochemical
208 processes in the reservoir. Biogeochemical processes occurring in the Three Gorges
209 Reservoir may be responsible for the $p\text{CO}_2$ over-saturation at TPX, HL and YC (Abil
210 et al., 2013; Algesten et al., 2005; Brothers et al., 2012; McDonald et al., 2013;
211 Weyhenmey et al., 2015). Thus, $\delta^{13}\text{C}_{\text{DIC}}$ values were significantly and negatively
212 correlated to increasing discharge (Fig. 4b).

213

214 Relationships between $p\text{CO}_2$ and organic carbon concentration

215 Transformation between inorganic and organic forms of carbon will alter the
216 $p\text{CO}_2$ in inland waters. When terrestrial or autochthonous organic carbon is
217 mineralized, CO_2 is produced in the reservoir (Kosten et al., 2010), while
218 phytoplankton productivity will remove CO_2 from the water (Wang et al., 2015).
219 Although there was no relation between $p\text{CO}_2$ and discharge at QX, The $p\text{CO}_2$ values
220 at HL and YC were positively related to the DOC concentration (Fig. 5a and 5b),
221 which is similar to the results of Larsen et al., (2011) and Sobek et al., (2005). CO_2
222 over-saturation at HL and YC may be derived from the degradation of DOC in
223 high-flow. DOC is largely in the form of allochthonous C, and terrigenous C is an
224 important form of total C in the inland waters (Hope et al., 1996; Striegl et al., 2001;
225 Whitfield et al., 2010). In spite of the low contents, allochthonous DOC
226 mineralization may be an important driver of CO_2 over-saturation. Although there is
227 no marked spatial variation of DOC in the Three Gorges Reservoir areas, allothogenic
228 DOC inputs should counteract the effect of DOC degradation. Intense photosynthesis
229 and submerged respiration would induce both high DOC and $p\text{CO}_2$ concentrations in
230 the high-flow season.

231 Particulate organic carbon (POC) can be present at high concentration within the
232 Three Gorges Reservoir system and is strongly related to the concentration of total
233 suspended matter (TSM). TSM in surface waters of the Changjiang main stream
234 ranged from 0.9 to 123.6 mgL^{-1} . The relationship between POC% ($\text{POC}/\text{TSM} \times 100\%$)
235 and Total Suspended Matters (TSM) followed that found previously (Zhang et al.,

236 2014) showing the power-law function: $POC\%=16.59\times TSM^{(-0.57)}$ for samples
237 collected both upstream and downstream. The same pattern in both upstream and
238 downstream sites indicated that the Three Gorges Reservoir did not have a major
239 effect on the relationship between POC% and TSM (Fig. 6a).

240 There was a significant positive correlation between pCO_2 concentration and
241 POC were found at HL and YC (Fig. 6b), indicating that POC mineralization may be
242 a source of pCO_2 over-saturation in the Three Gorges Reservoir. Large amounts of
243 POC were present at high discharge in the high-flow season. At the same time, the
244 POC mineralization increased in the high-flow season with high POC concentrations
245 contributing to the pCO_2 over-saturation. Dai and Liu (2013); Xu and Milliman
246 (2009); Yang et al. (2014); Yang et al. (2007b) have found that the Three Gorges
247 Reservoir traps the sediment noticeably. The contribution from sediment respiration to
248 summer CO_2 emission is significant for boreal and subarctic lakes (Algesten et al.,
249 2005). So it is difficult to qualify the contribution of POC decomposition for water
250 pCO_2 over-saturation. However, these results are consistent with other studies that
251 show mineralization and degradation of organic carbon is a main driver of pCO_2
252 over-saturation (Algesten et al., 2005; Hope et al., 1996; Sobek et al., 2005; Ward et
253 al., 2013; Weyhenmeyer et al., 2012; Whitfield et al., 2010).

254 In recent years, isotope proxies application has become invaluable in studying
255 the riverine carbon cycle (Tamooh et al., 2013). $\delta^{13}C_{DIC}$ signatures have been used to
256 trace DIC sources, transport and transformation in inland waters based on the distinct
257 isotopic values of various carbon sources (Barth et al., 2003; Goodwin et al., 2016; Li

258 et al., 2010; Tamooh et al., 2013; Zhong et al., 2017). Riverine $\delta^{13}\text{C}_{\text{DIC}}$ dynamics are
259 primarily controlled by both chemical weathering in the catchment and
260 biogeochemical processes in inland waters. In general, carbonate weathering and
261 biological CO_2 dissolution are two primary DIC sources, and photosynthesis, calcite
262 precipitation and CO_2 degassing are primary mechanisms of DIC transformation and
263 loss. At QX, soil CO_2 discharge and organic carbon decomposition should be
264 responsible for the DIC temporal dynamics for the soil CO_2 contribution from various
265 tributaries (Zhong et al., 2017). Soil CO_2 discharge was related to the reactive contact
266 surface between water and soil. The soil CO_2 discharge would play a minor role in
267 DIC dynamics in the reservoir area, just because of the limited reactive surface of the
268 soil. Both $p\text{CO}_2$ and $\delta^{13}\text{C}_{\text{DIC}}$ are negatively correlated with increasing discharge (Fig.
269 2a and 2b). Although the soil CO_2 discharged into the river, the dilution effect on
270 $p\text{CO}_2$ can conceal the soil CO_2 discharge at QX.

271 Significant negative relationships between $\delta^{13}\text{C}_{\text{DIC}}$ and $p\text{CO}_2$ were presented in
272 HL and YC (Fig. 6). Relatively higher $p\text{CO}_2$ concentrations with lighter $\delta^{13}\text{C}_{\text{DIC}}$
273 values were occurred in high-flow. Although the stratification is not significant in the
274 reservoir area, the average residence time of water is from 6 to 30 days (Zhao et al.,
275 2013). Thus, there is enough time for degradation of organic carbon. The
276 over-saturation of $p\text{CO}_2$ in the Three Gorges Reservoir would result in out-gassing of
277 dissolved CO_2 to the atmosphere. However, there are minor spatial variations for the
278 water $p\text{CO}_2$. Inorganic carbon loading and organic carbon decomposition may be the
279 primary driver of $p\text{CO}_2$ in the Three Gorges Reservoir. Inorganic carbon loading

280 would shift to $\delta^{13}\text{C}$ -enriched DIC values, but the $\delta^{13}\text{C}_{\text{DIC}}$ values became more
281 negative at TPX, HL and YC than that at QX. Therefore, inorganic carbon loading
282 should not be regard as the primary driver of $p\text{CO}_2$ in the Three Gorges Reservoir. In
283 general, the upper Changjiang catchment has C3 plant coverage, suggesting that the
284 organic carbon will be depleted in ^{13}C in terms of water DIC for Three Gorges
285 Reservoir. The water impoundment of the Three Gorges Reservoir would increase the
286 riverine water transit time. Although the Three Gorges Reservoir releases flood water
287 for the flood control in the high-flow season, the organic carbon increases with
288 increased discharge, and mineralization and degradation of organic carbon likely
289 contributes to elevated dissolved CO_2 (Whitfield et al., 2010). The biological CO_2
290 dissolution would shift the $\delta^{13}\text{C}_{\text{DIC}}$ to negative values. The relations of $\delta^{13}\text{C}_{\text{DIC}}$ versus
291 $p\text{CO}_2$ are consistent with our hypothesis that organic carbon decomposition, depleted
292 in ^{13}C , is responsible for the water $p\text{CO}_2$ over-saturation in the reservoir (Fig. 7).
293 Therefore, the $p\text{CO}_2$ over-saturation in the Three Gorges Reservoir can be mainly
294 elucidated as that soil CO_2 recharge for the inflowing water and mineralization and
295 degradation of organic carbon in the reservoir area was the primary driver of CO_2
296 over-saturation.

297

298 Sensitivity of Temperature for $p\text{CO}_2$ in the TGR

299 Mineralization and degradation of organic carbon and primary productivity is
300 sensitive to temperature (Acuna et al., 2008; Maberly et al., 2013; Sobek et al., 2005),
301 which would regulate the water $p\text{CO}_2$. Negative relationship between $p\text{CO}_2$ and T was

302 found in QX, but the explained variance in $p\text{CO}_2$ by T was low ($R^2=0.135$, Fig. 8a).
303 Due to the turbid and fast-flow water for the QX, especially in high-flow, the $p\text{CO}_2$
304 dynamics cannot be elucidated by primary production. As discussed above, dilution
305 effects of $p\text{CO}_2$ and soil CO_2 recharge with inflowing of tributaries should control the
306 $p\text{CO}_2$ dynamics. Therefore, temperature is not the primary driver of $p\text{CO}_2$
307 over-saturation at this site. The $p\text{CO}_2$ concentration increased with increasing T for
308 TPX, HL and YC (Fig. 8b, 8c and 8d), supporting the hypothesis that lower ratios of
309 primary production than organic carbon mineralization was occurred in the reservoir.
310 High temperature stimulated high organic carbon mineralization rates, thus increasing
311 the water $p\text{CO}_2$. Therefore, organic carbon degradation and mineralization should be
312 responsible for the water $p\text{CO}_2$ over-saturation, and high temperature is the primary
313 driver of organic carbon mineralization.

314 $p\text{CO}_2$ in the waters is the main driver of CO_2 emission for inland waters.
315 Mineralization of organic carbon is the main source for replenishing the dissolved
316 CO_2 lost to the atmosphere or taken up by phytoplankton. The $p\text{CO}_2$ decreased along
317 the main stream for the Three Gorges Reservoir area in the low-flow season (Fig. 2a),
318 which should be ascribed to the aquatic CO_2 emission and low organic carbon
319 mineralization rates with low T. The $p\text{CO}_2$ increased along the main stream for the
320 Three Gorges Reservoir area in the high-flow season (Fig. 2a), indicating that the CO_2
321 produced by organic carbon mineralization is much higher than that lost as CO_2
322 emission to the atmosphere. Therefore, organic carbon mineralization is the primary
323 driver of CO_2 over-saturation with respect to the atmosphere for Three Gorges

324 Reservoir.

325

326 **Acknowledgements:**

327 This work is financially supported by the National Key R&D Program of China
328 through Grant Nos. 2016YFA0601002, National Natural Science Foundation of China
329 (Grant Nos. 41422303, 41571130072 and 41130536), and program from IAEA
330 (Contract No. 18442 in CRP of F33021). Stephen Maberly's work is supported by the
331 UK Natural Environment Research Council.

332

333 Abril, G et al. 2013. Wood decomposition in Amazonian hydropower reservoirs: An additional source
334 of greenhouse gases. *Journal of South American Earth Sciences*, 44: 104-107.

335 Acuna, V, Wolf, A, Uehlinger, U, Tockner, K. 2008. Temperature dependence of stream benthic
336 respiration in an Alpine river network under global warming. *Freshwater Biology*, 53(10):
337 2076-2088.

338 Algesten, G et al. 2005. Contribution of sediment respiration to summer CO₂ emission from low
339 productive boreal and subarctic lakes. *Microb Ecol*, 50(4): 529-35.

340 Aucour, A-M, Sheppard, SMF, Guyomar, O, Wattelet, J. 1999. Use of ¹³C to trace origin and cycling of
341 inorganic carbon in the Rhône river system. *Chemical Geology*, 159(1-4): 87-105.

342 Bao, H, Wu, Y, Zhang, J, Deng, B, He, Q. 2014. Composition and flux of suspended organic matter in
343 the middle and lower reaches of the Changjiang (Yangtze River) - impact of the Three Gorges
344 Dam and the role of tributaries and channel erosion. *Hydrological Processes*, 28(3):
345 1137-1147.

346 Barros, N et al. 2011. Carbon emission from hydroelectric reservoirs linked to reservoir age and
347 latitude. *Nature Geoscience*, 4(9): 593-596.

348 Barth, JAC, Cronin, AA, Dunlop, J, Kalin, RM. 2003. Influence of carbonates on the riverine carbon
349 cycle in an anthropogenically dominated catchment basin: evidence from major elements and
350 stable carbon isotopes in the Lagan River (N. Ireland). *Chemical Geology*, 200(3-4): 203-216.

351 Brothers, MS, Prairie TY, Giogio, PA. 2012. Benthic and pelagic sources of carbon dioxide in boreal
352 lakes and a young reservoir (Eastmain-1) in eastern Canada. *Global Biogeochemical Cycles*,
353 26, GB1002, doi:10.1029/2011GB004074.

354 Chen, H et al. 2011. Methane emissions from the surface of the Three Gorges Reservoir. *Journal of*
355 *Geophysical Research: Atmospheres*, 116(D21).

356 Dai, ZJ, Liu, JT. 2013. Impacts of large dams on downstream fluvial sedimentation: An example of the
357 Three Gorges Dam (TGD) on the Changjiang (Yangtze River). *Journal of Hydrology*, 480:
358 10-18.

359 Deng, K et al. 2016. Three Gorges Dam alters the Changjiang (Yangtze) river water cycle in the dry
360 seasons: Evidence from H-O isotopes. *Sci Total Environ*, 562: 89-97.

361 Goodwin, A et al. 2016. Species-specific imprint of the phytoplankton assemblage on carbon isotopes
362 and the carbon cycle in Lake Kinneret, Israel. *Inland Waters*, 6(2): 211-223.

363 Guo, J, Wang, F, Vogt, RD, Zhang, Y, Liu, CQ. 2015. Anthropogenically enhanced chemical weathering
364 and carbon evasion in the Yangtze Basin. *Sci Rep*, 5: 11941.

365 Hope, D, Kratz, TK, Riera, JL. 1996. Relationship between P_{CO_2} and Dissolved Organic Carbon in
366 Northern Wisconsin Lakes. *Journal of Environmental Quality*, 25: 1442-1445.

367 Humborg, C, Ittekkot, V, Cociasu, A, VonBodungen, B. 1997. Effect of Danube River dam on Black
368 Sea biogeochemistry and ecosystem structure. *Nature*, 386(6623): 385-388.

369 Johnson, MS et al. 2008. CO₂ efflux from Amazonian headwater streams represents a significant fate
370 for deep soil respiration. *Geophysical Research Letters*, 35(17).

371 Kosten, S et al. 2010. Climate-dependent CO₂ emissions from lakes. *Global Biogeochemical Cycles*,
372 24(2): n/a-n/a.

373 Larsen, S, Andersen, T, Hessen, DO. 2011. The pCO_2 in boreal lakes: Organic carbon as a universal
374 predictor? *Global Biogeochemical Cycles*, 25(2): n/a-n/a.

375 Li, C et al. 2016. Damming effect on the Changjiang (Yangtze River) river water cycle based on stable
376 hydrogen and oxygen isotopic records. *Journal of Geochemical Exploration*, 165: 125-133.

377 Li, SL et al. 2010. Geochemistry of dissolved inorganic carbon and carbonate weathering in a small
378 typical karstic catchment of Southwest China: Isotopic and chemical constraints. *Chemical*
379 *Geology*, 277(3-4): 301-309.

380 Maberly, SC, Barker, PA, Stott, AW, De Ville, MM. 2013. Catchment productivity controls CO₂
381 emissions from lakes. *Nature Climate Change*, 3(4): 391-394.

382 Mao, R, Chen, H, Li, S. 2017. Phosphorus availability as a primary control of dissolved organic carbon
383 biodegradation in the tributaries of the Yangtze River in the Three Gorges Reservoir Region.
384 *Sci Total Environ*, 574: 1472-1476.

385 Marcé, R et al. 2015. Carbonate weathering as a driver of CO₂ supersaturation in lakes. *Nature*
386 *Geoscience*, 8(2): 107-111.

387 McDonald, CP, Stets, EG, Striegl, RG, Butman, D. 2013. Inorganic carbon loading as a primary driver
388 of dissolved carbon dioxide concentrations in the lakes and reservoirs of the contiguous
389 United States. *Global Biogeochemical Cycles*, 27(2): 285-295.

390 Meybeck, M. 1982. Carbon, nitrogen, and phosphorus transport by World Rivers. *American Journal of*
391 *Science*, 282: 401-405.

392 Raymond, PA et al. 2013. Global carbon dioxide emissions from inland waters. *Nature*, 503(7476):
393 355-9.

394 Raymond, PA, Oh, NH, Turner, RE, Broussard, W. 2008. Anthropogenically enhanced fluxes of water
395 and carbon from the Mississippi River. *Nature*, 451(7177): 449-52.

396 Regnier, P. 2013. Anthropogenic perturbation of the carbon fluxes from land to ocean. *Nature*
397 *Geoscience*.

398 Sobek, S, Tranvik, LJ, Cole, JJ. 2005. Temperature independence of carbon dioxide supersaturation in
399 global lakes. *Global Biogeochemical Cycles*, 19(2): n/a-n/a.

400 Striegl, RG et al. 2001. Carbon Dioxide Partial Pressure and ¹³C Content of North Temperate and
401 Boreal Lakes at Spring Ice Melt. *Limnology and Oceanography*, 46(4): 941-945.

402 Tamooh, F et al. 2013. Dynamics of dissolved inorganic carbon and aquatic metabolism in the Tana
403 River basin, Kenya. *Biogeosciences*, 10(11): 6911-6928.

404 Wang, B, Liu, C-Q, Wang, F, Liu, X-L, Wang, Z-L. 2014a. A decrease in pH downstream from the

405 hydroelectric dam in relation to the carbon biogeochemical cycle. *Environmental Earth*
406 *Sciences*, 73(9): 5299-5306.

407 Wang, BL, Liu, CQ, Peng, X, Wang, FS. 2013. Mechanisms controlling the carbon stable isotope
408 composition of phytoplankton in karst reservoirs. *Journal of Limnology*, 72(1): 127-139.

409 Wang, F et al. 2011. Disrupting the riverine DIC cycling by series hydropower exploitation in Karstic
410 area. *Applied Geochemistry*, 45: 3827-3834.

411 Wang, FS et al. 2011. Carbon dioxide emission from surface water in cascade reservoir-riversystem
412 on the Maotiao River, southwest of China. *Atmospheric Environment*, 103: 129-137.

413 Wang, FS et al. 2015. Seasonal variation of CO₂ diffusion flux from a large subtropical reservoir in
414 East China. *Atmospheric Environment*, 103: 129-137.

415 Wang, FS, Liu, CQ, Wang, BL, Yu, YX, Liu, XL. 2014b. Influence of a reservoir chain on the transport
416 of riverine inorganic carbon in the karst area. *Environmental Earth Sciences*, 72(5):
417 1465-1477.

418 Ward, ND et al. 2013. Degradation of terrestrially derived macromolecules in the Amazon River.
419 *Nature Geoscience*, 6(7): 530-533.

420 Weyhenmeyer, GA, Kortelainen, P, Sobek, S, Müller, R, Rantakari, M. 2012. Carbon Dioxide in Boreal
421 Surface Waters: A Comparison of Lakes and Streams. *Ecosystems*, 15(8): 1295-1307.

422 Whitfield, CJ, Seibert, TA, Aherne, J, Watmough, SA. 2010. Carbon dioxide supersaturation in
423 peatland waters and its contribution to atmospheric efflux from downstream boreal lakes.
424 *Journal of Geophysical Research-Biogeosciences*, 115(G4).

425 Wu, QX, Han, GL, Tang, Y. 2012. Temporal and spatial variation of water chemistry and dissolved
426 inorganic carbon isotope characterization in Three Gorges Reservoir. *Acta Scientiae*
427 *Circumstantiae*, 32(3): 654-661.

428 Xu, KH, Milliman, JD. 2009. Seasonal variations of sediment discharge from the Yangtze River before
429 and after impoundment of the Three Gorges Dam. *Geomorphology*, 104(3-4): 276-283.

430 Yang, SL et al. 2014. Downstream sedimentary and geomorphic impacts of the Three Gorges Dam on
431 the Yangtze River. *Earth-Science Reviews*, 138: 469-486.

432 Yang, SL, Xu, KH, Milliman, JD, Yang, HF, Wu, CS. 2015. Decline of Yangtze River water and
433 sediment discharge: Impact from natural and anthropogenic changes. *Sci Rep*, 5: 12581.

434 Yang, SL, Zhang, J, Dai, SB, Li, M, Xu, XJ. 2007a. Effect of deposition and erosion within the main
435 river channel and large lakes on sediment delivery to the estuary of the Yangtze River. *Journal*
436 *of Geophysical Research*, 112(F2).

437 Yang, SL, Zhang, J, Xu, XJ. 2007b. Influence of the Three Gorges Dam on downstream delivery of
438 sediment and its environmental implications, Yangtze River. *Geophysical Research Letters*,
439 34(10).

440 Yu, H, Wu, Y, Zhang, J, Deng, B, Zhu, Z. 2011. Impact of extreme drought and the Three Gorges Dam
441 on transport of particulate terrestrial organic carbon in the Changjiang (Yangtze) River.
442 *Journal of Geophysical Research*, 116(F4).

443 Zhang, L et al. 2014. The spatiotemporal distribution of dissolved inorganic and organic carbon in the
444 main stem of the Changjiang (Yangtze) River and the effect of the Three Gorges Reservoir.
445 *Journal of Geophysical Research: Biogeosciences*, 119(5): 741-757.

446 Zhao, Y, Wu, BF, Zeng, Y. 2013. Spatial and temporal patterns of greenhouse gas emissions from Three
447 Gorges Reservoir of China. *Biogeosciences*, 10(2): 1219-1230.

448 Zhong, J, Li, SL, Tao, F, Yue, F, Liu, CQ. 2017. Sensitivity of chemical weathering and dissolved

449 carbon dynamics to hydrological conditions in a typical karst river. *Sci Rep*, 7: 42944.

450

451

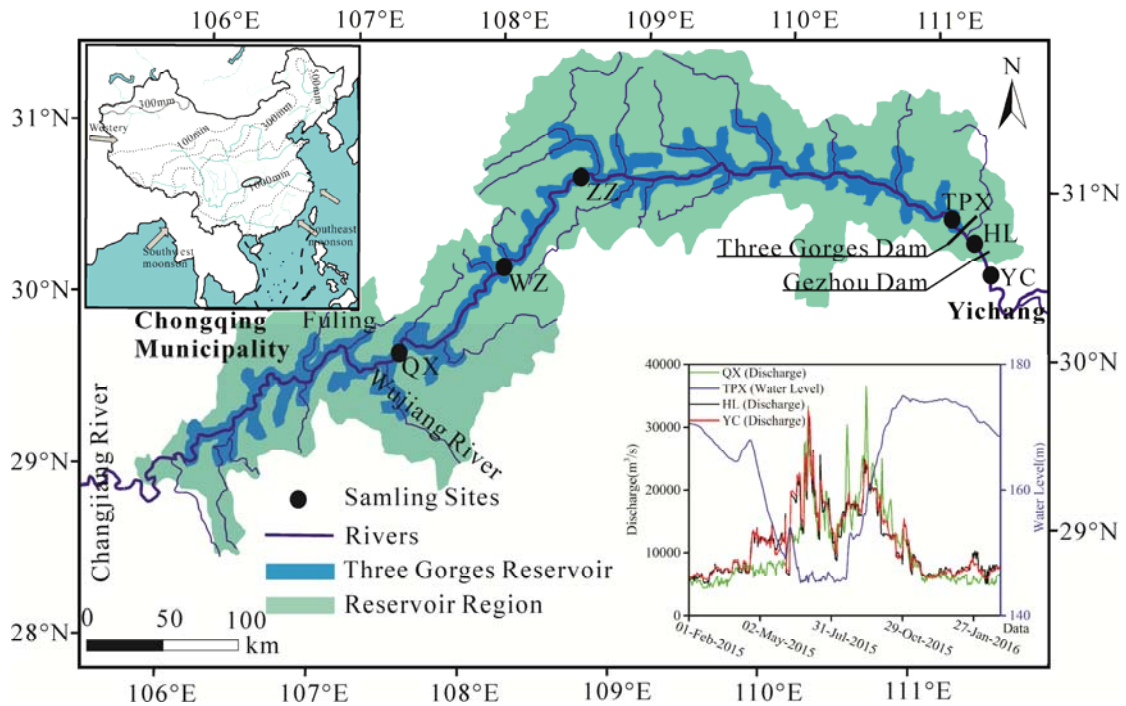


Figure. 1 The location of sampling sites in the Three Gorges Reservoir area. The sampling sites are at Qingxi (QX), Wanzhou (WZ), Zhongzhou (ZZ), Taipingxi (TPX), Huanglingmiao (HL) and Yichang (YC). The upper inset shows the location of the region within China and the lower inset shows discharge at QX, HL, YC, as well as water level at TPX for February, 2015 to February, 2016.

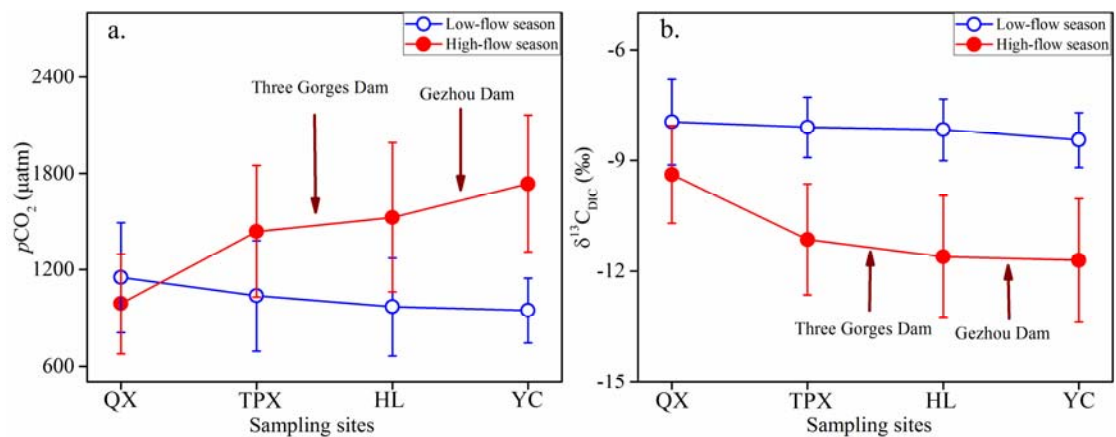


Figure. 2. Changes in $p\text{CO}_2$ and $\delta^{13}\text{C}$ at four sites along the Three Gorges Reservoir system at low and high flow. a. Variation in $p\text{CO}_2$; b. variation in $\delta^{13}\text{C}_{\text{DIC}}$. Average of all samples in each season is shown along with standard deviation.

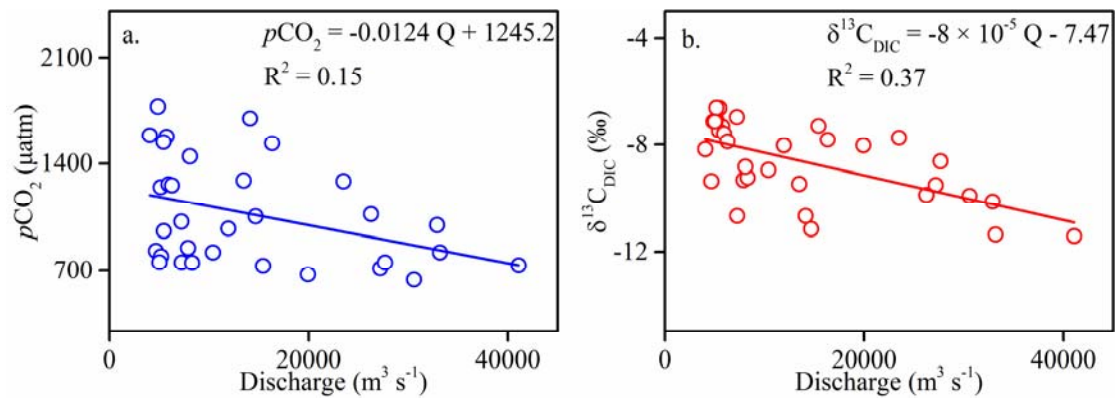


Figure 3. The relationship between $p\text{CO}_2$ or $\delta^{13}\text{C}_{\text{DIC}}$ and discharge at the upstream site on the Three Gorges reservoir Qingxi (QX). a. $p\text{CO}_2$ versus discharge; b. $\delta^{13}\text{C}_{\text{DIC}}$ versus discharge.

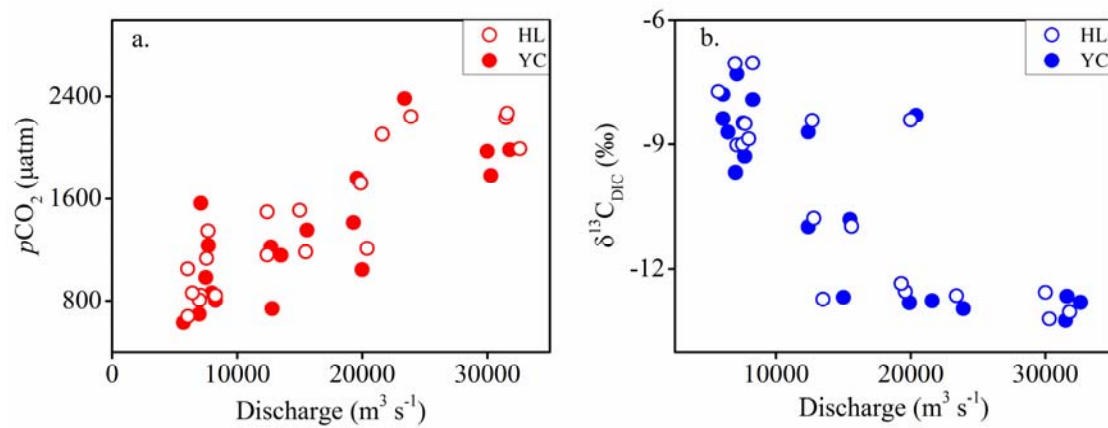


Figure 4. The relationship between $p\text{CO}_2$ or $\delta^{13}\text{C}_{\text{DIC}}$ and discharge at Huanglingmiao (HL) and Yichang (YC). a. $p\text{CO}_2$ versus discharge; b. $\delta^{13}\text{C}_{\text{DIC}}$ versus discharge.

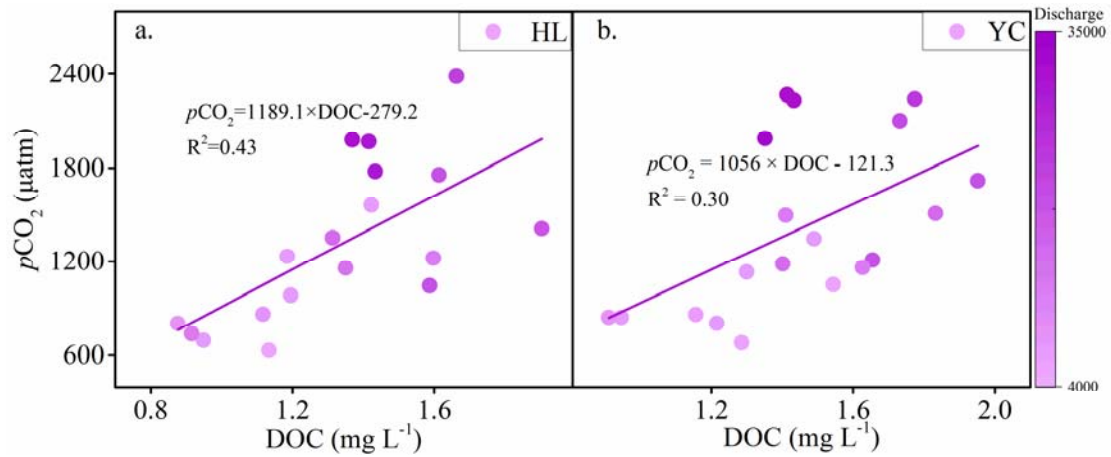


Figure. 5 Correlation between $p\text{CO}_2$ and concentration of DOC at Huanglingmiao (HL) (a) and Yichang (YC) (b) Discharge ($\text{m}^3 \text{s}^{-1}$) is indicated by the density of the symbol.

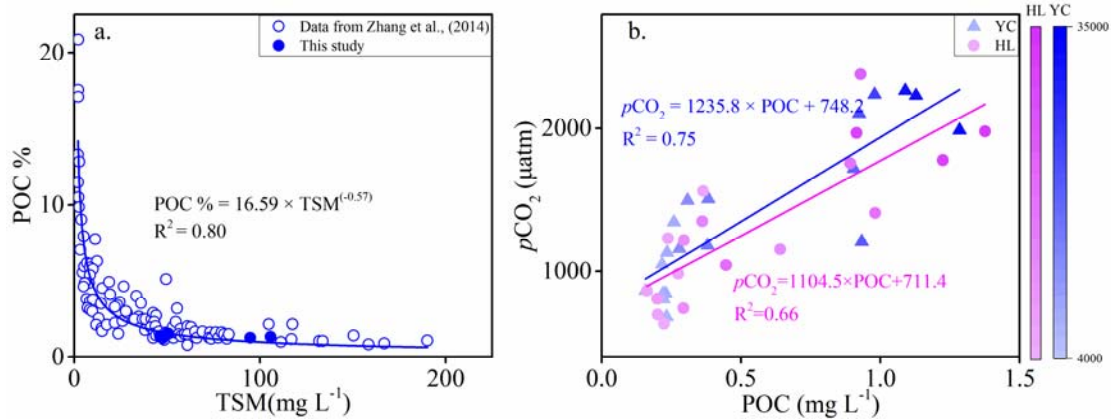


Figure. 6a. Relationships between POC and TSM or $p\text{CO}_2$ in the main stem of the Changjiang River. a. Relationship between POC% and TSM at this study in comparison to data from Zhang et al. (2014); b. Relationship between $p\text{CO}_2$ and POC at Huanglingmiao (HL) and Yichang (YC). Discharge ($\text{m}^3 \text{s}^{-1}$) is indicated by the density of the symbol.

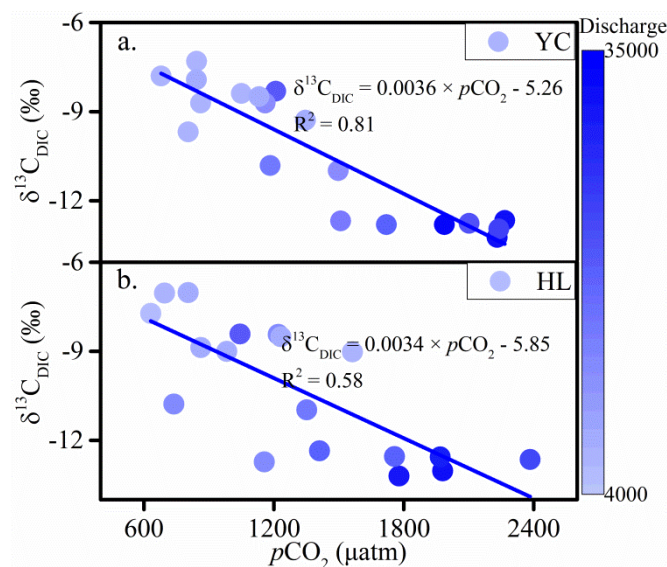


Figure. 7. Correlation between $\delta^{13}\text{C}_{\text{DIC}}$ and $p\text{CO}_2$ at a. Yichang (YC) and b. Huanglingmiao (HL). Discharge ($\text{m}^3 \text{s}^{-1}$) is indicated by the density of the symbol.

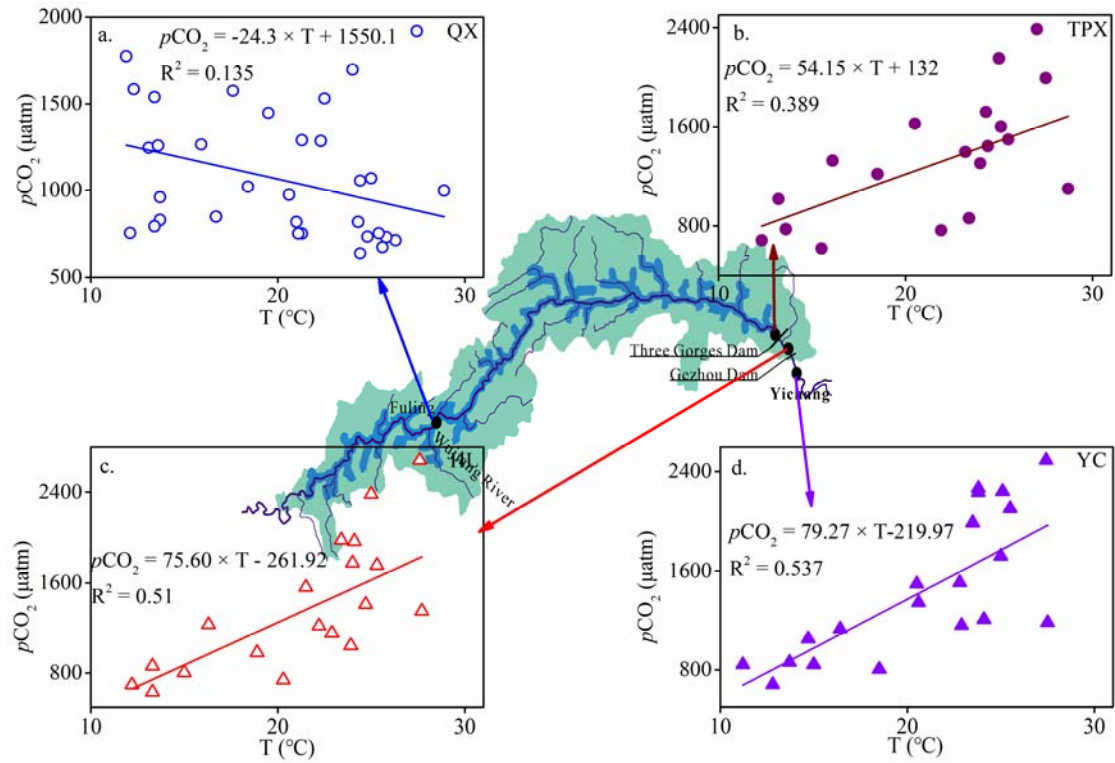


Figure. 8. Scatter plot of $p\text{CO}_2$ versus water temperature at: a. Qingxi (QX), b. Taipingxi (TPX), c. Huanglingmiao (HL) and d. Yichang (YC).